The first spectroscopic analysis of Ethiopian prehistoric rock painting

Cristiana Lofrumento,[a]* Marilena Ricci,[b] Luca Bachechi,[c] Denise De Feo[d] and Emilio Mario Castellucci[e]

An extensive micro-Raman spectroscopic study of prehistoric rock paintings found in Hararghe region, Ethiopia, was carried out, with the aim to evaluate the production skill of the local artist and the period of production of the discovered paintings. Attenuated Total Reflection Fourier Transform Infrared (ATR-FTIR) Spectroscopy and Laser Induced Breakdown Spectroscopy (LIBS) were used as auxiliary techniques. Micro sampling were carried out on parts of red, white, black painting figures representing domestic and wild animals. The pigments used by artists were hematite for red color, calcite or gypsum for white color, and carbonaceous material for black coloration. A green pigment was also investigated; it resulted made of green earth. A consistent amount of Ca-oxalate was found particularly on red samples as well as on the white ones. Former studies attributed oxalates origin to a biological substrate attack, whereas in the present case Ca-oxalate is ascribed to the use of an organic stuff to spread properly the pigments on the substrate.Principal Component Analysis was performed on the hematite spectra; it evinced that the spectral features could be indicative of different sites and of the relative age.1These novel evaluations put into new perspective the knowledge about rock art pictorial technology of the Horn of Africa. Copyright © 2011 John Wiley & Sons, Ltd.

Supporting information may be found in the online version of this article.

Keywords: Raman mapping; rock art; Africa; oxalate

Introduction

The Hararghe region is in the east central area of Ethiopia; it is an enclave in the inner part of the Oromya region. The major concentration of the whole Ethiopian prehistoric rock painting examples was found within its territory. In fact, there are a great number of archaeologically interesting sites located in this region, as shown in Fig. 1. They represent a considerable artistic heritage and are comprised of sites, most of which are sheltered, situated both in caves and open tracts of land (Fig. 2). They were found in the first half of the 20th century, and since then they have been extensively described and studied.

Prehistoric Ethiopian rock art has found expression essentially through two forms: paintings and engravings, which are present to different extents in two distinct areas of the country. The first zone is in the South, in the region between the Great Rift Lakes and the border with Kenya, whereas the second one is in the East, in the administrative region of Hararghe. At the moment, in the Southern part of the country, sites with engravings are prevalent, while in the Eastern zone of Ethiopia the engravings are very rare, whereas cave paintings are widespread.

From 1842, the year of the first discovery of rock art in the Horn of Africa,[1] until the present, hundreds of artistic testimonies that attest to the existence of very different styles and techniques have been identified in this geographic area, under shelters or on caves walls. The majority of the sites show patterns referring to domestic animals (Fig. S1), in particular to cattle, while in some localities only depictions of wild fauna were found. However, despite this richness and a variety of artistic expressions, paradoxically, art from the Horn of Africa is still today largely unknown.

There are currently two fundamental issues regarding Ethiopian rock art that require careful attention: the chronology of its development at various sites and its possible significance on an African and world scale. The attribution of a chronological order to Ethiopian rock art is a demanding undertaking, because the data information that can be inferred from the archaeological documentation is extremely fragmentary. The few details available of absolutely verified chronology are insufficient to establish a time series that is somehow correlated to the artistic events. At present, the solution of the chronological problem is thus particularly necessary, because it still relies only on accurate observation and stylistic comparison that enabled the definition of the so-called the Ethiopian–Arabic artistic movement to be made. This movement, active between the fifth and the fourth millennium BP, suggested a probable chronological position of the rock art expression between the end of the third and the second millennium BC,[2] because of the stylistic affinities with the material culture[3] and the Nubian C-Group art.[4]

With regard to the significance of this art, there are two main interpretative lines based on the literature available. It could

* Correspondence to: Cristiana Lofrumento, University of Florence, Chemistry, Sesto Fiorentino, Italy. E-mail: cristiana.lofrumento@unifi.it

a University of Florence, Chemistry, Sesto Fiorentino, Italy

b University of Florence, Contructions and Restoration, Florence, Italy

c University of Florence, Science of the Antiquity, Middle Ages and Renaissance and Linguistics, Florence, Italy

d Chemistry, Sesto Fiorentino, Italy

e Universita di Firenze, Chemistry, Sesto Fiorentino, Toscana, Italy

Figure 1. Map of the Hararghe region, with the positioning of the archaeological sites: 1. Barru Qabanawa, Dadabe, Goda Hattu, Mhuganawa, Woddo; 2. Goda Burqa, Karre Geldesa; 3. Goda Ajewa, Goda Dubata, Karre Sura; 4. Goda Baboo, Goda Busa, Goda Gayaa, Goda Gawra Bejil; 5. Deka Keteba II, Goda Haban Sofi, Goda Wenji; 6. East Stinico, Errer Kimiet I, Errer Kimiet II, Saka Sharifa.

either represent only an exquisitely aesthetic product or, alternatively, the paintings could signify a magical manipulation of the material or spiritual world through producing images. The present consensus is that the topologic and stylistic interpretation of the artistic heritage of the Horn of Africa seems to pertain to a more prosaic context. The images show events from everyday life represented by scenes in a simplistic and basic way. The rock art from this part of Africa seems to be just the product of a pastoral world at the threshold of history, evolving gradually towards more complex social forms.

The study of Ethiopian rock art is therefore only at its beginning, and the documentation referring to this type of artistic expression is still much too limited with respect to the vastness of the territory. Nevertheless, the activity of the past fifteen years has been particularly important as it has resulted in the discovery of many new art documents.

In the above described scenario, the analysis of the chemical composition of the paintings constitutes an important instrument aimed at the acquisition of data that could be of considerable help

in the study of rock art paintings. It could prove, for example, the existence of affinities, among the different sites, because of the use of palettes with similar pigments. It could also identify the presence of materials helpful for radiocarbon dating.

Experimental

Techniques

The optical techniques used in this research study on the Hararghe rock art paintings were applied to determine the coloring material used as pigments and to search for organic substances, probably employed as binders.

Micro-Raman analyses on the Hararghe rock art samples were executed to determine the coloring material used as pigments and to search for organic material, whereas FT-IR spectroscopy in the attenuated total reflectance (ATR) procedure was applied as an investigation technique for the comparison with micro-Raman spectroscopy to obtain greater information about the whole
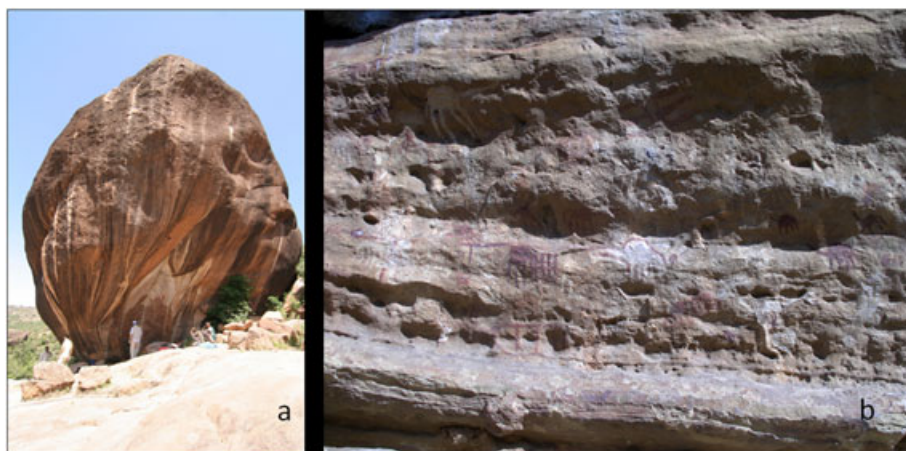

Figure 2. View of two archaeological sites: (a) Saka Sharifa and (b) Goda Ajewa.

materials of the 65 analyzed specimens. The ATR technique allows a global and general acknowledgment of the investigated sample, which is examined in full.

A further help comes from laser-induced breakdown spectroscopy (LIBS) analyses, which was crucial to exclude the presence of iron and manganese in black samples, thus ascertain the sole use of carbonaceous material for dark colors.

Micro-Raman analyses were performed by means of a Renishaw RM 2000 apparatus equipped with an Argon ion laser, emitting light at 514.5 nm, and a diode one, with a 785 nm wavelength. The laser power at the samples was within the range 4 mW–400 μW when using the diode laser and in the 2 mW–140 μW range for the Argon ion laser. Microscope objectives of different magnification ($\times 5$, $\times 20$, $\times 50$, $\times 100$) were used to preliminarily observe the morphology of the samples by white light, while the $\times 50$ magnification objective was utilized to focus the laser beam on the sample surface to acquire the spectrum. The theoretical spatial resolution was 1.3 μm when using the diode laser, and 0.8 μm for the Argon ion one; the spectral resolution was 2 cm^{-1} and 6 cm^{-1} for the diode and the Argon ion laser, respectively.

Attenuated total reflectance-FTIR spectra were recorded by a Perkin Elmer Spectrum 100 spectrophotometer. The reflection system (the universal attenuated total reflectance) consisted of a diamond crystal, a flat focusing lens made of KRS-5, and a movable device applying on the sample a pressure aimed at eliminating air. The detector was fast recovery deuterate L-alanina tryglicine sulfate at a Peltier effect stabilized temperature. The spectral resolution was 4 cm^{-1}; the investigated spectral range was 380–4500 cm^{-1}.

For LIBS analyses, a compact nanosecond Q-switched Nd:YAG s, and their broadenin. The acquisition laser (model CFR 200-GRM, Big Sky Lasers, 8 ns, 20 Hz, $0.005 - 115$ mJ/pulse for the 532 nm emission) was used as irradiation source. The light emitted from the sample was collected through the same lens that was used to focus the laser beam, and was subsequently focused into a 0.30 m imaging spectrograph (model SP-2358i, Acton Research) equipped with three interchangeable diffraction gratings with 150, 300, and 1200 grooves/mm. The ICCD was a detector with 1024×256 imaging pixels (model P.I. Max-1024/RB-PTG, Princeton Instruments) and a minimum gate speed of 1 ns.[5]

Samples

The analyzed samples were carefully drawn from 64 rock painting sites, most of them recently discovered in Ethiopia. The samples were removed with extreme care and they were taken with minimum effect on the paintings and their surrounding area. They have reduced size, from about ten microns to some millimeters. Some of them were in powder form, whereas the others consisted of very small fragments.

Some samples from the raw and without paintings rock were also taken to get information on compounds that may have been added, which could be related to the possible use of a binder to properly spread pigments on the pictorial substrate.

The numbered samples and their corresponding color and their provenance site name, are reported in Table 1.

All the samples come from shelters. In some cases, for example for Woddo, the paintings are completely outdoors, because the shelter does not exist anymore, so they are weather-beaten.

Results and Discussion

Micro-Raman analyses on the samples themselves furnished satisfactory results with regard to inorganic substances, such as pigments, but less information on the presence of organic materials. This is the reason why the study was then carried out by means

Table 1. Analyzed samples divided for numbering, stylistic chronological attribution, color, and provenance sites

Sample	Color	Provenance site	Sample	Color	Provenance site	Sample	Color	Provenance site
1 Probably old	Red	East Stinico	23 old	Red	Goda Gawra Bejil	43 recent	Red	West Stinico
2 Old	Red	Deka Keteba II	24 contemporary	White		44 recent	Black	
3 Old	Red	Karre Sura	25 old	Black		45 recent	White	
4 Old	Red		26	Rock		46	Rock	
5 Old	Red		27 old	Red	Goda Baboo	47 old	Red	Goda Hattu
6 Intermediate	Red	Goda Ajewa	28 old	Black		48	Rock	
7 Intermediate	White		29 old	White		49 old	White	Errer Kimiet II
8 Old	Red	Errer Kimiet I	30 contemporary	White		50	Rock	
9 Old	White		31	Rock		51 old	Red	Woddo
10 Contemporary	White		32 old	Red	Karre Geldesa	52 old	Red	
11 Old	Light red		33 old	Black		53	Rock	
12 Old	Deep red		34	Rock		54 recent	Green	
13 Contemporary	Black	Saka Sharifa	35 old	White	Goda Busa	55 recent	Red	Mhuganawa
14 Old	Orange		36 recent	Gray		56 recent	White	
15 Old	Red		37 recent	Red	Goda Burqa	57 recent	Red	Dadabe
16 Old	Black	Goda Wenji	38 recent	Black		58 recent	Red	
17 Old	Red		39	Rock		59 recent	White	
18 Old	Red	Goda Gayaa	40 old	Red	Goda Dubata	60	Rock	
19	Rock		41 old	Black		61	Rock	
20 recent	Red	Goda Haban Sofi	42	Rock		62 old	Red	Barru Qabanawa
21 recent	White					63 old	White	
22	Rock					64	Rock	

of ATR-FTIR spectroscopy, which was helpful to gain additional information.

Obviously, we cannot compare exactly the results obtained by the two techniques, ATR-FTIR and micro-Raman, because of the substrate heterogeneity, but they can be considered as helpful additional information for a complete characterization of the studied rock paintings.

Red pigments

Most samples showed red coloring, commonly used in the majority of prehistoric rock paintings. Red sample surfaces were quite patchy, because of the presence of red, white, and grey particles.

Spectra acquired on white and grey crystallites, which were irradiated by means of a 50× objective, revealed the presence of gypsum (strongest band at 1007 cm^{-1}), quartz (strongest band at 465 cm^{-1}) and, for a few specimens, of calcite (strongest band at 1089 cm^{-1}).

All the red grains exhibit the Raman features of hematite, the α form of ferric oxide (α–Fe$_2$O$_3$)[6–8] present in red ochre; however, usually bands of calcium oxalate appear together with the hematite ones in the different spectra of the red pigment. Hematite is the pigment almost always employed in prehistoric paintings[9,10] and its spectrum displays the features corresponding to the Raman active vibrational modes of this oxide (Fig. 3), where the 500 cm^{-1} peak is attributable to the vibrational mode A$_{1g}$, while the ones at 294, 410, 612 cm^{-1} to the E$_g$ ones.[11]

Figure 3 shows some hematite spectra acquired corresponding to red grains on reddish painted samples, where four of the seven predicted Raman active first-order modes of hematite are observed. They show a broad band at about 660–670 cm^{-1}, which was previously assigned to the presence of residual magnetite or maghemite (γ–Fe$_2$O$_3$) contamination, normally occurring in association with hematite or kaolinite in natural ochre.[12] Previous works,[6,13–17] concerning the heating of the hematite powder well above the temperature at which magnetite and maghemite are known to undergo complete thermal transformation to hematite in the presence of air, led to the conclusion that the peak at about 660 cm^{-1} can be due to an IR active longitudinal optical (LO) E$_u$ mode, visible in Raman spectra thanks to the lowering of symmetry occurring in disordered structures, such as ochre [18–21] or in doped hematite, such as the Al-bearing hematite.[11]

As long as the hematite spectrum may give useful information about stoichiometry, composition, and atom substitutions existing in iron oxide structures,[22] Raman spectra on five different points per sample were registered on some of the red specimens
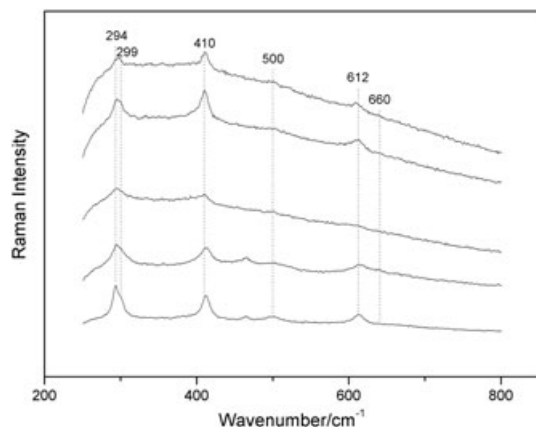
to evaluate if any characterizing difference would have occurred through principal components analysis (PCA). PCA is a powerful statistical method that reduces the dimensionality of a data matrix by generating a new set of orthogonal variables, called principal components.[23,24] Principal components are new and perpendicular axes in space; they are displaced on the axes of the maximum of data variance. In Raman spectroscopy, the shift, disappearance, and appearance of certain Raman peaks have been used for the determination of the phase transition region in iron oxides with good accuracy.

Samples 2, 5, 20, 37, 43, 51, 55, 62 were taken into consideration for these further analyses; samples 2, 5, 51, 62 were classified, on the basis of iconographical and stylistic criteria, and of the colors overlapping, as 'old', whereas the others as 'new', because they are attributed to recent paintings (Fig. S2). The spectra were acquired by irradiating the samples, by means of a 50× magnification objective, with a diode laser (785 nm), and a power of 3.8 mW on the irradiated surface. Even if such a high laser power leads to a shift of Raman bands towards low wavenumbers and a band broadening,[11] it was used to obtain an intensity increasing of the hematite bands (Fig. S3) to better evaluate their relative positions, and their broadening.

The acquisition time was 30 s per spectrum, with five accumulations. With the aim of assessing the Raman spectrum of the mere iron oxide, only the intensity corresponding to the wavenumbers in the 260–750 cm^{-1} range were taken into account; the lower limit (260 cm^{-1}) is imposed by the not optimal cut of the notch filter for the removal of the elastic component feature. PCA was carried out by performing an area normalization of the hematite Raman spectra to have at our disposal a scaled matrix of data referring to the hematite spectra.

Principal components analysis plots are very helpful to highlight differences between 'old' red samples and the 'recent' ones. Actually, the PCA scores plot shows two groups referring to old (red points) and recent (green points) samples, almost completely separated along the first principal component (PC1), which alone is able to explain 80% of the data variance (Fig. 4).

A better understanding of the spectral characteristics influencing the old/recent grouping comes from the loadings plot referring to PC1 and the second principal component (PC2) (Fig. 5).

This graph shows positive high weights referred to both PC1 and PC2 in the 260–440 cm^{-1} and 594–632 cm^{-1} ranges, where the main bands of hematite are present (the 292, 410, and 610 cm^{-1} ones). Important information comes from the PC1 loadings plot, showing a shoulder at about 390 cm^{-1} of the 410 cm^{-1}

Figure 3. Raman spectra of hematite acquired on different red grains.
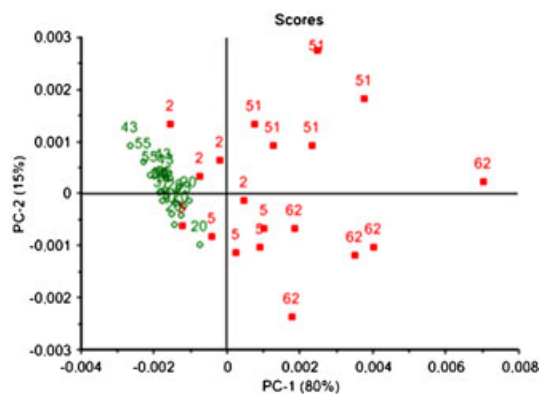

Figure 4. Scores plot referred to red samples spectra. Square-points correspond to samples from 'old' sites, while the circular ones to the 'recent' sites.
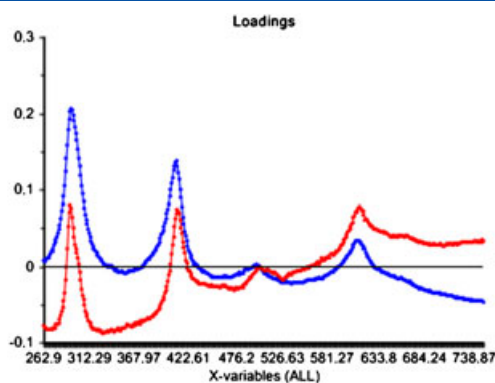
Figure 5. Loadings plot of red samples spectra referring to PC1 (upper spectrum) and PC2 (lower spectrum).

hematite band. This could suggest that samples with positive values on the PC1 coordinate, are not constituted of hematite alone, although they exhibit a certain goethite (α–FeOOH) or, in general, limonite (hydrated iron oxides, frequently associated with hematite weathering[25]) content.

A further grouping of the analyzed samples would come from the feature at about 660 cm^{-1}, which can be observed on the PC2 loadings plot. It could be indicative of the different sites of the samples. Even if it is well known that a variety of different shades of yellow and red color could be obtained simply by heating goethite,[26–28] which turns into hematite at temperatures in the range of ~260–280 °C,[29] a previous work[31] demonstrated that Raman spectroscopy cannot be used to differentiate heated goethite from natural hematite, in spite of being effective in making a distinction between ordered hematite from the disordered one. As a consequence of that, an interesting issue regards the feature that contributes to a great degree to PC2, arising from the loadings in the range 636–687 cm^{-1}. This spectral region, as mentioned above, shows a peak at approximately 660 cm^{-1} in the Raman spectrum of disordered hematite.[30] The importance of this band resides in the fact that it is not present in the spectrum of pure, hence ordered, hematite or/and of hematite obtained from goethite heated at temperatures higher than 1000 °C;[29,31] therefore, it could be used as a means of the samples characterization on the basis of the order degree of hematite itself.

Besides hematite, goethite was also found in various samples, even if in scant quantity; it was in the form of small yellow grains. Goethite is a ferric hydroxide (α–FeOOH), very common in prehistoric rock art. Intimate mixture of different iron-containing phases may be indicative of the heating technological process, already known in prehistoric times, for which goethite was used to obtain hematite,[32] otherwise the two minerals might have been extracted from a mining deposit containing both of them.[22]

The presence of iron oxides, particularly hematite, was confirmed in all the red samples, together with gypsum and/or calcite.

Black pigments

The relative Raman spectra acquired on different points of black samples evidenced the carbon-containing compound presence by means of the characteristic two broad features G (graphitic, 1580 cm^{-1}) and D1 (disorder, 1320 cm^{-1}), respectively assigned to crystalline graphite and to structural disorder in the graphitic structure[33] (Fig. S4). Many researchers report on the Raman character of the natural organic matter in carbon-containing compounds, such as coal, and relate the Raman bands to the

structural order of the amorphous carbons. The basis of most of these studies evolved around the assignment of the G (graphitic, ~1580 cm^{-1}) band to crystalline graphite and any other bands, called D bands, (disorder, various from 1100 to 1500 cm^{-1}) to any type of structural disorder in the graphitic structure.

Laser-induced breakdown spectroscopy analyses were performed to exclude the presence of iron and manganese, thus confirming the carbonaceous nature of black pigments.

The use of carbonaceous material as black pigment in Ethiopian rock paintings evidences a different pictorial technique with respect to that employed in the rock art sites not far from them; in fact the characterization of painting materials from Eritrea rock art sites shows the use of manganese hydro-oxides in black paints by means of micro-Raman analysis.[34]

White pigments

The application of white pigments is probably the most recent; it could be significant for the attempt of the age attribution of the paintings of different sites (Fig. S5). White pigments coming from the supposed 'contemporary' sites are constituted by calcite alone, whereas the ones from the 'old' sites contain both calcite and gypsum (Fig. 6). It is not possible to state if the real composition of the old white pigments utilized for the paintings was a mixture of calcite and gypsum like in the Catamarcan cave-paintings[35] or the nearer Eritrean sites.[34] This doubt is due to the fact that calcium sulfate originates also from the sulfation process to which calcite might be subjected because of weathering;[36] nevertheless, the scant amount of gypsum corresponding to the rock samples may suggest its use as a pigment.

Green pigments

A surprising result comes from the green pigment of sample nr.54 (Fig. S6). Raman spectra evidenced that the coloring is due to the mineral celadonite,[37] indicating an early use of green earth in African rock art (Fig. 6). It could be considered the evidence that predates its use, if considering the pre-Hispanic polychrome pictograph from the Chumash Indian site of San Emigdio, California.[38]

Organic materials

The Raman spectra acquired on samples nr.10, 28, 40 by diode laser present a feature because of the use of an organic pictorial
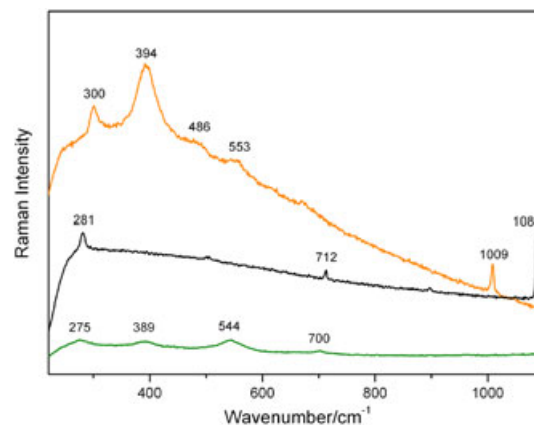

Figure 6. Raman spectrum of yellow, white, and green pigments, shown respectively from the bottom to the top.

medium. A further analysis on the sample nr.10, belonging to a more recent period with respect to the other samples of the Errer Kimiet I site, was performed with argon laser, and it confirmed the presence of beeswax, evidenced by the Raman feature at 2853 and 2884 cm^{-1} (Fig. S7). [39]

Also, ATR-FTIR results evidenced the presence of organic matter, with a spectrum very similar to the beeswax one (Fig. 7),[40,41] together with the presence of the monohydrated form of Ca-oxalate.

Even if beeswax has been dated back up to 4000 BP,[42] the very intense IR peaks referred to the active vibrational modes in beeswax in the analyzed sample may be attributed to its use in recent times as a polisher, probably by indigenous people to make the pictograph more vivid.

Oxalates

Calcium oxalate, in the monohydrated form (whewellite) was found by Raman microscopy on almost all the pigmented areas of the paintings, especially on the red ones. The presence of Ca-oxalate may be considered a clue of some degradation phenomena occurring in artworks.

Attenuated total reflectance-FTIR analysis also gave results on the rocky substratum in agreement with the micro-Raman ones, showing the characteristic features of calcite, quartz besides those of silicates.

The monohydrated calcium oxalate (CaC_2O_4–H_2O) is observable in the IR spectra of the samples. In Fig. 8 some typical calcium oxalate bands are visible: the peak at 1623 cm^{-1}, ascribable to the H_2O bending, the one at 1325 cm^{-1}, because of the C–O–C stretching, together with the other bands at 784, 670,[43] and the ones corresponding to the OH stretching near 3400 cm^{-1}.

In previous studies on rock art, the presence of Ca-oxalates was ascribed to biological attacks of algae, fungi or lichens, inducing fungal hyphae to penetrate and to leave oxalates as a product of their metabolism;[35,44–46] this evaluation originated from the observation of compact patinas on the substratum and accretions. Hernanz *et al.* proposed a biological mechanism for the formation of Ca oxalate layers, i.e. the result of the metabolism of fungi and lichens that colonizes rocks, e.g. *Verrucaria nigrescens*.[8,46] However, they attribute the observed sandstone weathering process to the crystallization of gypsum in the sandstone pores of the rock surface.[8,46] On the contrary, Hedges *et al.*[47] explained
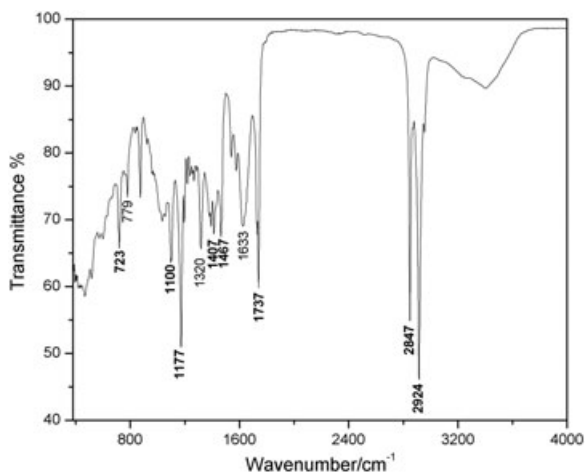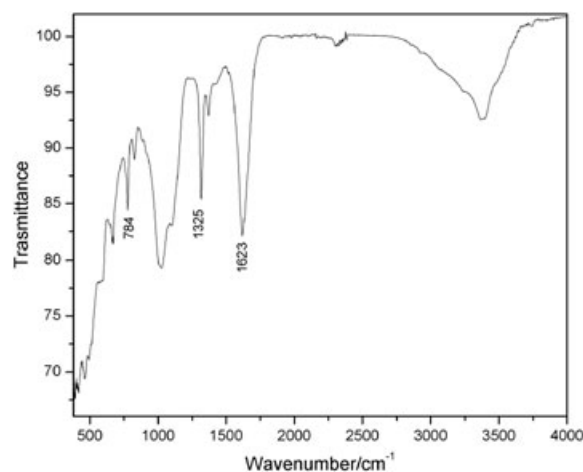

Figure 8. ATR-FTIR spectrum of sample nr.9. In the figure the vibrational wavenumbers of Ca-oxalate are reported.

that Ca-oxalate could be deliberately collected to compose the pigment, as a consequence of the highly different amount of whewellite observed in the pigment samples with respect to nonpainted samples from the same cave. A further source of oxalic acid has been ascribed also to the presence of rock hyraces in shelters.[48,49]

With the aim of trying to understand the origin of Ca-oxalates, Raman analyses were performed also on samples obtained from raw rock without paintings for the following sites: Goda Gayaa, Goda Haban Sofi, Goda Gawra Bejil, Goda Baboo, Karre Geldesa, Goda Burqa, Goda Dubata, West Stinico, Goda Hattu, Errer Kimiet II, Woddo, and Barru Qabanawa. The spectra acquired on raw rock show that Ca-oxalate is present in scant quantity, thus suggesting its intentional addition corresponding to the painted areas, and excluding that it could be deposited naturally. A confirmation of such a hypothesis comes from the Raman mapping image of the displacement of Ca-oxalate on a red fragment compared with the Raman mapping of the hematite area (Fig. 9).

Figure 9 clearly displays that Ca-oxalate does not form a compact and homogeneous layer on the red pigmented surface; on the contrary it appears scattered and rarefied on the hematite stratum. This observation could lead to the hypothesis that an organic binder was used mixed with pigments to make them adhere to the rock substratum. The supposed organic material should have contained a source of oxalic acid, which would have reacted with a Ca-based pigment, and subsequently formed Ca-oxalate, because it is generally envisaged that one does not foresee finding organic dyestuffs or plant extracts used in ancient rock art, the latter being susceptible to attack by adverse or unfavorable microclimates pertaining to caves and shelters.

Some research works[47,50–52] suggested the use of vegetable substances in the prehistoric rock art, that is to say that substances extracted from plants were employed as binders and sometimes as dyes or some parts of the plants were utilized to apply the pigments to the support.

There are numerous plant species that are able to produce Ca-oxalate crystals, with different biological functions, which collect in the cellular tissue. Because the vegetation of Eastern Ethiopia is constituted mostly of succulent plants, we considered the hypothesis that plant sap, obtained by squeezing out or pressing leaves and stalks, could have been employed to dilute pigments so that as time passed, only Ca-oxalate crystal could
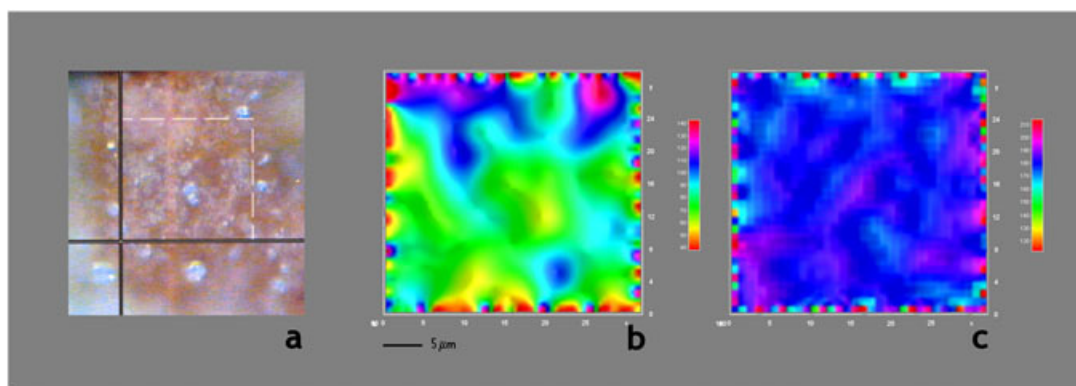

Figure 7. ATR-FTIR spectrum of sample nr.10. The figure shows the vibrational frequencies of beeswax (bold font) and Ca-oxalate.

Figure 9. (a) Image of the analyzed area of red sample nr. 20 (×50 objective); (b) Raman mapping of Ca-oxalate; and (c) Raman mapping of hematite.

reveal the use of such types of binders. With the aim of testing the possibility of evaluating the presence of Ca-oxalate in the juice of a typical succulent plant by means of Raman microspectroscopy, we treated a cladode of nopal plant with the procedure described by Malainine *et al.*[53] The nopal plant (*Opuntia ficus*, or *Opuntia ficus-indica*) has evolved morphological and physiological characteristics as a response to scarcity of water, extreme variations of temperature and in general to the harsh conditions of arid and semi-arid regions. It is present in large amounts in the proximity of the considered rock art sites.

An important remark regarding the appearance of the substance extracted from the nopal cladode is that it is viscous and sticky before filtration and suspension in a NaOH solution, and transparent once desiccated; these are the distinctive features for a good binder.

Micro-Raman analyses on the extracted stuff confirmed the presence of Ca-oxalate crystals, as evidenced by the Raman spectrum acquired on a white crystal (Fig. 10). The presence of Ca-oxalate was evaluated by means of many different techniques,[54–56] but to our knowledge not yet by micro-Raman spectroscopy.

Nopal plant was chosen arbitrarily as a species from which to extract Ca-oxalate crystals, because of its considerable availability. This does not exclude the use of sap from different plants, extracted, for example, from the plant present in the surroundings. Even nowadays Hararghe natives extract the latex from these plants to use it as mastic.[57]

A previous study[58] evidenced that the stronger reactivity of calcium carbonate, related to its high solubility in acids, with

respect to calcium sulfate, leads to an easier transformation into calcium oxalate, even at low oxalic acid concentrations, which is comparable to that of plants; on the contrary Fe-oxalate did not form in any of the treated samples, even at high oxalic acid concentration solutions. Hence, the contemporary presence of calcium sulfate, calcium carbonate, and calcium oxalate corresponding to the pigmented areas could be considered as a clue of a pigment/calcium pigment/binder (containing oxalic acid) mixture.

Most probably, different binders were used for red and white colorings with respect to the black ones, because a lesser amount of Ca-oxalate was found in correspondence with the dark colored areas. The carbonaceous material could also have been obtained by a process provoking the consumption of the binder itself.

Conclusions

The results obtained in the present study have highlighted some important issues regarding rock art pictorial technique. The use of organic binders to better apply pigments on the proper substrate was evidenced through Raman compositional maps, which were very helpful to visualize the scattered distribution of the Ca-oxalate grains throughout the red colored samples. This is in contrast to the former hypothesis of a supposed Ca-oxalate origin from a biological attack, because the Hararghe specimens do not show a compact Ca-oxalate layer on their surface. The origin of Ca-oxalate on the surface of the Hararghe rock paintings could come from the regrounding of the pigment mixed with some sort of binder to give it permanence. The type of binders that would have served the purpose could be the ones, all readily available at the time, containing a source of oxalic acid of Ca-oxalate itself, such as animal oils, blood, egg white, urine, honey or casein, but most probably vegetable oils or juices from the plants.

It was possible to describe also the palette of the local artists; it was constituted of hematite, mixed with the white pigment calcite for red, calcite for white, whereas carbonaceous material was used for black coloration. The origin of gypsum is not very clear, because of the fact that it could arise from calcite as an alteration product or used as pigment.

Another aspect to take into consideration is that the accurate examination of the Raman spectra registered in correspondence of hematite grains on different samples may furnish a clue both of the different site provenance, as suggested by the performed PCA analysis, and of the age of the paintings, whose evaluation could be carried out by considering that in the 'recent' sites a
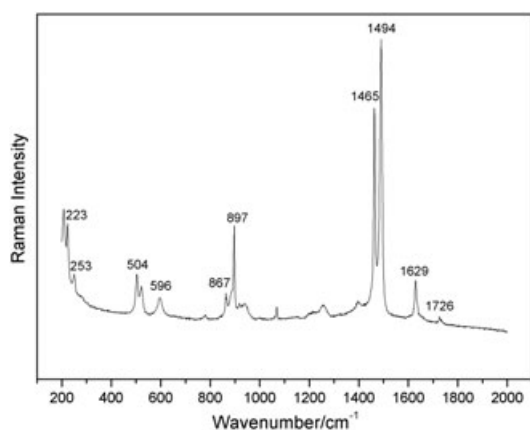

Figure 10. Raman spectrum of the white precipitate obtained from the nopal cladode extraction.

better crystallized and pure hematite was used, with respect to the one from the 'old' sites.

An absolute chronological collocation attempt could be estimated through radiocarbon dating, as beeswax, carbonaceous material, and calcium carbonate represents an important carbon source.

Supporting Information

Supporting information may be found in the online version of this article.

References

[1] A. d'Abbadie, *Bulletin del la Sociètè de Geographie* **1842**, *XVII*, 2.
[2] R. Joussaume, *Préhistoire Africaine*. Mélanges offerts au Doyen Lionel Balout, A.P.D.F., Paris, **1981**, 159.
[3] S. A. Brandt, N. Carder, *World Archaeol.* **1987**, *19*, 194.
[4] P. Červiček, *Rassegna di studi etiopici* **1978–79**, *XXVII*, 5.
[5] I. Osticioli, N. F. C. Mendes, A. Nevin, A. Zoppi, C. Lofrumento, M. Becucci, E. M. Castellucci, *Rev. Sci. Instrum.* **2009**, *80*, 076109.
[6] D. L. A. de Faria, S. V. Silva, M. T. de Oliveira, *J. Raman Spectrosc.* **1997**, *28*, 873.
[7] H. G. M. Edwards, D. W. Farwell, E. M. Newton, F. Rull Perez, S. Jorge Villar, *J. Raman Spectrosc.* **2000**, *31*, 407.
[8] A. Hernanz, J. M. Gavira-Vallejo, J. F. Ruiz-López, H. G. M. Edwards, *J. Raman Spectrosc.* **2008**, *39*, 972.
[9] H. G. M. Edwards, L. Drummond, J. Russ, *J. Raman Spectrosc.* **1999**, *30*, 421.
[10] D. C. Smith, M. Bouchard, M. Lorblanchet, *J. Raman Spectrosc.* **1999**, *30*, 347.
[11] A. Zoppi, C. Lofrumento, E. M. Castellucci, Ph. Sciau, *J. Raman Spectrosc.* **2008**, *39*, 40.
[12] D. Bikiaris, S. Daniilia, O. Katsimbiri, E. Pavlidou, A. P. Moutsatsou, V. Chryssoulakis, *Spectrochim. Acta, part A* **1999**, *56*, 3.
[13] R. M. Cornell, U. Schwertmann, *The iron oxides: structure, properties, reactions, occurrences, and uses* (2nd edn), Wiley-VCH, Weinheim, **2003**.
[14] O. N. Shebanova, P. Lazor, *J. Raman Spectrosc.* **2003**, *34*, 845.
[15] J. van der Weerd, G. D. Smith, S. Firth, R. J. H. Clark, *J. Archaeol. Sci.* **2004**, *31*, 1429.
[16] X. Nie, X. Li, C. Du, Y. Huang, H. Du, *J. Raman Spectrosc.* **2008**, *40*, 76.
[17] M. Hanesch, *Geophys. J. Int.* **2009**, *177*, 941.
[18] K. F. McCarty, *Solid State Commun.* **1988**, *68*, 799.
[19] D. Bersani, P. P. Lottici, A. Montenero, *J. Raman Spectrosc.* **1999**, *30*, 355.
[20] J. Wang, W. B. White, J. H. Adair, *J. Am. Ceram. Soc.* **2005**, *88*, 3449.
[21] I. V. Chernyshova, M. F. Hochella, A. S. Madden, *Phys. Chem. Chem. Phys.* **2007**, *9*, 1736.
[22] F. Froment, A. Tournié, Ph. Colomban, *J. Raman Spectrosc.* **2008**, *39*, 560.
[23] S. Wold, K. Esbensen, P. Geladi, *Chemom. Intell. Lab. Syst.* **1987**, *2*, 37.
[24] J. E. Jackson, *A User's Guide to Principal Components*, John Wiley & Sons, Inc., New York, **1991**.
[25] C. Klein, C. S. Hurlbut Jr., *Manual of Mineralogy*, John Wiley, Florida, **1993**, 396.
[26] L. F. C. de Oliveira, H. G. M. Edwards, R. L. Frost, T. Kloprogge, P. S. Middleton, *Analyst* **2002**, *127*, 536.
[27] M. P. Pomiés, M. Menu, C. Vignaus, *Archaeometry* **1999**, *41*, 275.
[28] H. D. Ruan, R. L. Frost, J. T. Kloprogge, L. Duong, *Spectrochim. Acta, Part A* **2002**, *58*, 479.
[29] D. L. A. de Faria, F. N. Lopes, *Vib. Spectrosc.* **2007**, *45*, 117.
[30] A. M. Jubb, H. C. Allen, *ACS Appl. Mater. Interfaces* **2010**, *2*, 2804.
[31] S. Gialanella, F. Girardi, G. Ischia, I. Lonardelli, M. Mattarelli, M. Montagna, *J. Therm. Anal. Calorim.* **2010**, *103*, 867.
[32] M. P. Pomiés, M. Barbaza, M. Menu, C. Vignaud, *l'Anthropologie* **1999**, *3*,1.
[33] H. G. M. Edwards, E. M. Newton, S. O'Connor, D. Evans, *Anal. Bioanal. Chem.* **2010**, *397*, 2685.
[34] A. Zoppi, G. F. Signorini, F. Lucarelli, L. Bachechi, *J. Cult. Herit.* **2002**, *3*, 299.
[35] H. G. M. Edwards, E. M. Newton, J. Russ, *J. Mol. Struct.* **2000**, *550–551*, 245.
[36] F. Ospitali, A. Rattazzi, M. P. Colombini, A. Andreotti, G. Di Lonardo, *J. Cult. Herit.* **2007**, *8*, 323.
[37] F. Ospitali, D. Bersani, G. Di Lonardo, P. P. Lottici, *J. Raman Spectrosc.* **2008**, *39*, 1066.
[38] D. A. Scott, S. Scheerer, D. J. Reeves, *Stud. Conserv.* **2002**, *47*, 184.
[39] H. G. M. Edwards, D. W. Farwell, L. Daffner, *Spectrochim. Acta, part A* **1996**, *52*, 1639.
[40] B. Zimnicka, A. Hacura, *Pol. J. Environ. Stud.* **2006**, *15*, 112.
[41] A. M. Bakr, T. Kawiak, M. Pawlikowski, Z. Sawlowicz, *J. Cult. Herit.* **2005**, *6*, 351.
[42] D. E. Nelson, G. Chaloupka, C. Chippindale, M. S. Alderson, J. R. Southon, *Archaeometry* **1995**, *37*, 151.
[43] P. Maravelaki-Kalaitzaki, *Anal. Chim. Acta* **2005**, *532*, 187.
[44] A. Watchman, N. Cole, *Antiquity* **1992**, *67*, 335.
[45] A. Hernanz, J. F. Ruiz-López, J. M. Gavira-Vallejo, S. Martin, E. Gavrilenko, *J. Raman Spectrosc.* **2010**, *41*, 1394.
[46] A. Hernanz, J. M. Gavira-Vallejo, J. F. Ruiz- López, *J. Raman Spectrosc.* **2006**, *37*, 1054.
[47] R. E. M. Hedges, C. B. Ramsey, G. J. Van Klinken, P. B. Pettitt, C. Nielsen-Marsh, A. Etchegoyen, J. O. Fernandez Niello, M. T. Boschin, A. M. Llamazares, *Radiocarbon* **1998**, *40*, 35.
[48] L. C. Prinsloo, *J. Raman Spectrosc.* **2007**, *38*, 496.
[49] L. C. Prinsloo, W. Barnard, I. Meiklejohn, K. Hall, *J. Raman Spectrosc.* **2008**, *39*, 646.
[50] A. Watchman, *Antiquity* **1993**, *67*, 58.
[51] N. Cole, A. L. Watchman, *Rock Art Res.* **1992**, *9*, 27.
[52] J. M. Arocena, K. Hall, I. Meiklejohn, *Geoarchaeol.: Int. J.* **2008**, *23*, 293.
[53] M. E. Malainine, A. Dufresne, D. Dupeyre, *Verlag der Zeitschrift für Naturforschung Tübingen* **2003**, *58c*, 812.
[54] P. V. Monje, E. J. Baran, *Plant Physiol.* **2002**, *128*, 707.
[55] P. A. Nakata, *Plant Sci.* **2003**, *164*, 901.
[56] M. Contreras-Padilla, E. Pérez-Torrero, M. I. Hernández-Urbiola, G. Hernández-Quevedo, A. del Real, E. M. Rivera-Muñoz, M. E. Rodríguez-García, *J. Food Compos. Anal.* **2011**, *24*, 38.
[57] L. Bachechi, *Archivio per l'Antropologia e l'Etnologia* **2007**, *CXXXVII*, 249.
[58] A. Zoppi, C. Lofrumento, N. F. C. Mendes, E. M. Castellucci, *Anal. Bioanal. Chem.* **2010**, *397*, 841.